

Model-Based Validation Within the Rail-Wheel-Subgrade Modeling

Dirk Söffker¹, Svenja Kirchenkamp¹, and Peter C. Müller²

¹ Gerhard-Mercator University Duisburg, Dynamics and Control,
47048 Duisburg, Germany

² University of Wuppertal, Safety Control Engineering,
42097 Wuppertal, Germany

Abstract. This contribution presents the idea of model-based model validation. For this purpose the PI-Observer as core of a validation scheme is introduced. Task of this observer scheme is the estimation of unknown, unmeasured interaction effects within the considered system. Therefore it is assumed, that the whole system is divided in known and unknown parts. Estimating dynamic interaction effects inner ratios within the unknown part are reconstructed. This model-based reconstruction scheme can be used for validation purposes if real measurements are available.

As example the adhesion models are validated. The contact force highly depends on the kinematical contact situation and additionally on external effects. By observing the contact situation by the actual adhesion characteristic between rail and wheel can be determined.

As a first application example the simulations of the driven wheel show the strategy and the efficiency of this approach.

1 Motivation

For model validation by comparison of predicted with real values, measurements are needed. Here usually costly experimental validation especially for models with a wide application range are necessary. Further on model validation often is done using specific test-rigs to realize conditions to allow measurements, which typically can not be assigned to practical problems. Another problem is that measurements of the interesting system part and of the interaction effects to others are not available. This means that practical realization of measurements restricts the model refinements to those effects, which affects the output. The proposed method overcomes these difficulties by the application of a robust model-based technique which uses simple to realize measurements and model knowledge to predict inner values of unknown parts of the considered model.

The principle idea is illustrated by the validation of the nonlinear adhesion characteristic. The adhesion-friction micromechanism is the core of the transport mechanism of locomotion. Figure 1 gives possible contact situations of a rail-wheel contact. The area of an optimal use of the contact situation is defined due to the assumption of the maximum position of the friction-slip ratio on the left hand side of the maximum, if a maximum is available.

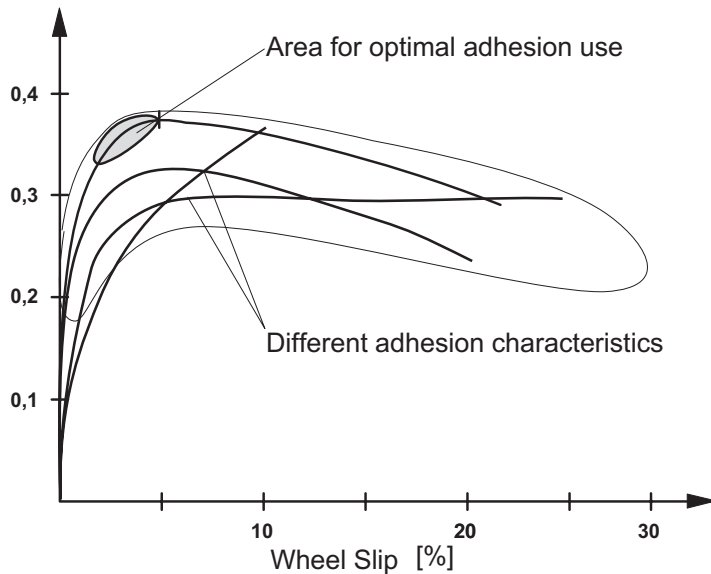


Fig. 1. Area of the optimal adhesion of the rail-wheel contact

The rail-wheel contact is highly nonlinear due to the complex geometrical contact problem and the unknown environment parameters (temperature et al.). Several papers focus to the modeling of the contact phenomena, trying to understand the effects as well [10], [21]. Furthermore the interaction between the elastic track, the elastic rail, the elastic contact itself and the wheel is of interest, because of several safety, economical and comfort aspects [18].

The problem of validation of those contact models are unavailable measurements of the contact area. The model-based model validation technique offers with the Proportional Integral (PI) Observer a possibility for validation in cases where measurements are impossible or too costly. The PI-Observer uses known model parts and easy available measurements from the known parts to estimate unknown effects within the unknown parts.

So it works as a 'virtual measurement device'. The method is illustrated in Fig. 2.

The aim of this contribution is to demonstrate the possibilities of observer-based estimation of nonlinear contact forces. Therefore it is not necessary to work with detailed models of the mechanical system itself rather than with arbitrary disturbed models to examine the robustness of the observer technique itself to its own model assumptions.

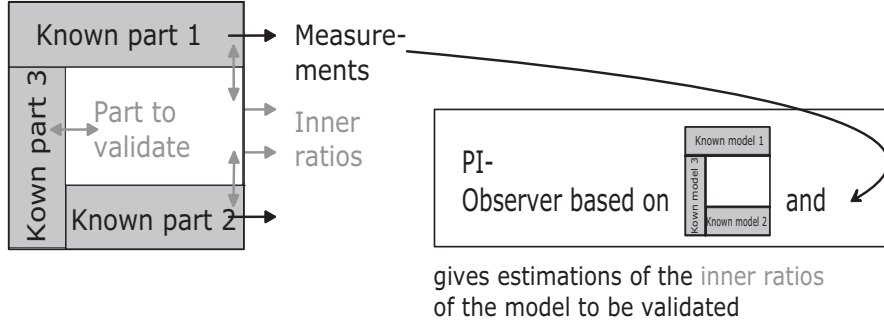


Fig. 2. The PI-Observer as a virtual measurement device

2 The Rail-Wheel Contact

Modeling of the contact between two elastic bodies is a classical problem. The solution to the normal-contact problem – the determination of the contact area and the planar pressure functions – was given by Hertz [6]. In this contribution the contact area is assumed as an ellipse, described by the radii a, b . This includes that the contact partners are shifted together with the distance

$$\delta = \left(\frac{N}{\sqrt{R_a}} 2 \frac{(1-\nu)}{G} \right)^{\frac{2}{3}} \alpha_a, \quad (1)$$

with N acting as normal force, R_a as wheel radius, ν as the contraction number ($= 0.3$ (steel)), the shear modulus G and the coefficient α_a . The ellipse radii are connected by

$$b = a\sqrt{1 - e^2} \quad (2)$$

(cf. [11]), where e defines the eccentricity of the contact ellipse. Relations between the radii R_a, R_b of the contact partners and the eccentricity are given by

$$\frac{R_b}{R_a} = \frac{(1 - e^2)D(e)}{B(e)} \quad (3)$$

(cf. [11]), with the coefficients $D(e), B(e)$ as solutions from elliptic integrals. Tabular solutions are given in [14].

In this contribution a dynamical contact is assumed, where the coefficients R_a, R_b, α_a are fixed. The coefficient α_a is chosen with $\alpha_a = 0.549$.

The contact force can be modeled assuming the theory of Kalker [9]. Here the tangential contact force is modeled using the model of Shen-Hedrick-Elkins [20]. Here only the tangential slip η is considered. The tangential contact force T_ξ is modeled by

$$T_\xi = \alpha T_\xi^{lin.} = -\alpha abGC_{11}\eta, \quad (4)$$

with

$$\alpha = 1 - \frac{1}{3} \left(\frac{T_{\xi}^{lin.}}{\mu N} \right) + \frac{1}{27} \left(\frac{T_{\xi}^{lin.}}{\mu N} \right)^2 \quad \text{for } T_{\xi}^{lin.} < 3\mu N \quad (5)$$

$$\alpha = \frac{\mu N}{T_{\xi}^{lin.}} \quad \text{for } T_{\xi}^{lin.} \geq 3\mu N, \quad (6)$$

and C_{11} as a Kalker coefficient which is chosen fixed. The equations (1)–(6) define a piecewise constant contact force / slip relation for the elastic contact. This simplified model is sufficient to show the efficiency of this approach.

3 The Proportional-Integral-Observer

In this paper a Proportional-Integral Observer (PIO) is used, which allows the robust estimation of modeled system states, additionally the estimation of unknown inputs in desired / interesting input channels. If the nominal system behaviour can be described by a nominal system description, changes in the system structure or of system parameters can be understood as additional external inputs acting to the nominal system and representing the fault. In contrast to the Extended Kalman Filter, this procedure considers the dynamical changes both of structure and parameter. In contrast to actual works about the Unknown Input Observer (UIO) [7], this approach works in an approximated wise, but with weak conditions.

In the sequel it can be shown that the PIO allows the robust estimation of such unknown inputs interpreted as disturbances to the nominal system. The main idea of this paper is the application of this observer type to nominal known systems for fault diagnosis, in the way that the operator of a dynamical system gets a new tool looking for inner, unmeasurable states of a system. Combining the estimations of the PIO a new quality of inner informations of the faulty structure is available. The main details of PIO is already given and proved in [23]. In this paper the PIO is extended for applications as Unknown-Input Observer (UIO), applied for estimation of unknown additive inputs, like the contact forces of the rail-wheel contact.

3.1 History of Disturbance Estimation

Based on a linear and deterministic description of the plant, which describes the nominal unfaulty dynamical behaviour of the plant, the Luenberger observer can reconstruct unmeasurable states using measurements of outputs. This permits the employment of the Luenberger-observer scheme to dynamic systems of the form

$$\dot{x} = Ax + Bu, \quad y = Cx, \quad (7)$$

with the state vector x of order n , the vector of measurements y of order r_1 , and the known input vector u of order m . The system matrix A , the input matrix B and the output matrix C are of appropriate dimensions. However, it is not directly applicable to nonlinear systems or systems with unknown inputs. Since the proposed type of observer beside the proportional feedback like the Luenberger-observer, also uses integral information of the estimation error, it is called PI-observer (PIO). It is known from literature, that the PI-observer design is useful for linear systems with constant disturbances [3]. Here the PI-observer is developed from another viewpoint. Continuing the ideas of Johnson [8], who introduced linear models for disturbances acting upon linear systems, and Müller [16], [17], who gave the conditions and proofs for modeling disturbances as linear models also acting upon linear systems, this paper deals with the idea of constructing a ‘disturbance model’ for more general use, especially to the practical case, in which no information about the disturbance, the structure of the fault resp., is available. Here the term ‘disturbance model’ describes the use of disturbance models describing the signal behaviour of external inputs regretted as disturbances, representing the disturbance rejection philosophy given in [8], [16] and [17]. Here this term is used only to relate the proposed development of the PI-observer to the known disturbance rejection strategy, which can be considered as a special case.

The following aspects are the points of consideration: usual Luenberger observer fails, if the system (7) is only roughly known or/and there exist additional unknown inputs caused by nonlinearities. Using known PI-observer techniques this disadvantage can be compensated, but only for piecewise constant disturbances [3]. If the unknown input is caused by modeling errors or unmodeled nonlinearities (unmodeled dynamics), this assumption is not fulfilled.

In the general case of an external input, which can not be described by a linear model extension (disturbance rejection theory), the system description (7) fails. Therefore, a more general description of such systems is given

$$\dot{x} = Ax + Bu + Nf(x, u, t), \quad y = Cx \quad . \quad (8)$$

In (8) the vector function $f(x, u, t)$ of dimension r_2 describes in general the nonlinearities caused by the external input, unknown inputs and unmodeled dynamics of the plant and may be a nonlinear function of states, control inputs and time. The matrix N is the corresponding distribution matrix locating the unknown inputs to the system. Without loss of generality here it is assumed that the matrices N, C have full rank.

Several successful practical and theoretical applications concerning machine diagnosis [22] and also observer-based control [2], [15] are known. In all of these cases an approximation

$$f \approx Hv \quad (9)$$

of the vector of nonlinearities f (friction torques, forces caused by the crack) was used. In the theory of DRC [8], [16], [17], the linear time-invariant system

with the unknown inputs Nf caused by nonlinearities, unknown inputs or unmodeled dynamics is described by the linear exo-system

$$\dot{v} = Fv \quad . \quad (10)$$

The resulting extended linear dynamical model includes these inputs and appears as

$$\begin{bmatrix} \dot{x} \\ \dot{v} \end{bmatrix} = \begin{bmatrix} A & NH \\ 0 & F \end{bmatrix} \begin{bmatrix} x \\ v \end{bmatrix} + \begin{bmatrix} B \\ 0 \end{bmatrix} u, \quad (11)$$

$$y = [C \ 0] \begin{bmatrix} x \\ v \end{bmatrix}, \quad (12)$$

and can be used as an (extended) base building up an extended linear observer. Here the matrix N relates the fictitious approximations Hv of the unknown inputs f to the states where they appear. The signal characteristics of these inputs will be approximated by a linear dynamical system with the system matrix F . Using the extended system description (11),(12) an extended observer can be designed, so the estimate \hat{v} of v represents the approximation of the disturbances, whereby \hat{x} is the estimation of x .

In the applications [22], [2], [15] it is noticed that using

$$F = 0, \quad F \rightarrow 0, [\text{resp.}] \quad (13)$$

leads to a very good reconstruction of the diagnosed nonlinearity. This means that without exact knowledge about the dynamical behaviour of the unknown inputs f ($F = 0$ represents a constant disturbance [3]), a very general approach is possible by assuming the disturbance as approximately piecewise constant (related to the ‘disturbance model’-philosophy), but applying the observer scheme to applications where this assumption is not fulfilled.

By the given procedure using ‘ $F = 0$ ’ in the sense of disturbance model philosophy, the successfully applied scheme appears as the PI-observer and will be seen as a natural comprehensible extension of the well known Luenberger observer [23].

Figure 3 shows the structure of the observer therefore (8) is written in the following form

$$\dot{x} = Ax + Bu + b + N^*n^*(x, t). \quad (14)$$

where b is the known input which is independent from u and N^*n^* describes the unknown, external inputs.

Here in contrast to the conventional Luenberger approach a second loop with two gain matrices L_2, L_3 and integrator is used additionally.

Now, the question is how to determine the matrices L_1, L_2 and L_3 such that the corresponding PIO works well. Therefore the estimation performance is analyzed for different cases of the dynamical behaviour of the unknown input related to the nominal system.

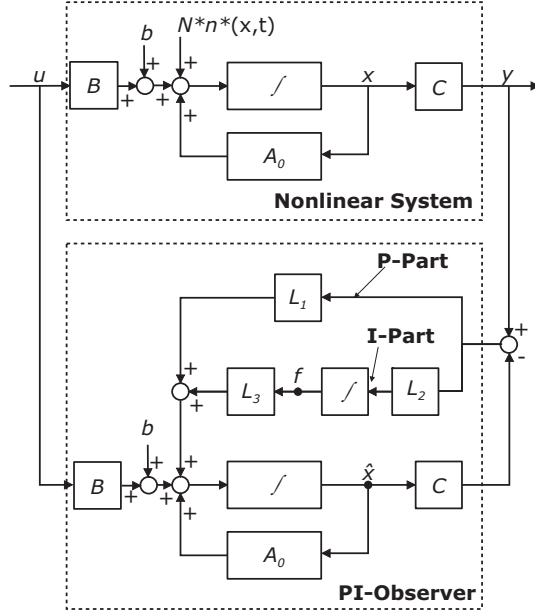


Fig. 3. Structure of the PI-Observer

3.2 Estimation Behavior

The development of the theory behind follows the works in [23], [26]. From the structure of the PI-observer depicted in Fig. 3 it follows, that the dynamics of PI-observer is described by

$$\dot{\hat{x}} = A\hat{x} + L_3\hat{f} + Bu + L_1(y - \hat{y}) \quad \dot{\hat{f}} = L_2(y - \hat{y}) \quad (15)$$

where $\hat{y} = C\hat{x}$. Writing (8) in a matrix form gives

$$\begin{bmatrix} \dot{\hat{x}} \\ \dot{\hat{f}} \end{bmatrix} = \begin{bmatrix} A & L_3 \\ 0 & 0 \end{bmatrix} \begin{bmatrix} \hat{x} \\ \hat{f} \end{bmatrix} + \begin{bmatrix} B \\ 0 \end{bmatrix} u + \begin{bmatrix} L_1 \\ L_2 \end{bmatrix} (y - \hat{y}) \quad (16)$$

or

$$\begin{bmatrix} \dot{\hat{x}} \\ \dot{\hat{f}} \end{bmatrix} = \underbrace{\begin{bmatrix} A - L_1C & L_3 \\ -L_2C & 0 \end{bmatrix}}_{A_e} \begin{bmatrix} \hat{x} \\ \hat{f} \end{bmatrix} + \begin{bmatrix} B \\ 0 \end{bmatrix} u + \begin{bmatrix} L_1 \\ L_2 \end{bmatrix} y. \quad (17)$$

Now the problem is how to design the gain matrices L_1 , L_2 , and L_3 , such that the observer can estimate approximately the states x of the plant.

Defining the estimation error as $e(t) = \hat{x}(t) - x(t)$. Then, from (7), (8) and (17) we have that

$$\begin{bmatrix} \dot{e} \\ \dot{\hat{f}} \end{bmatrix} = A_e \begin{bmatrix} e \\ \hat{f} \end{bmatrix} \quad (18)$$

in the case of system (7), or

$$\begin{bmatrix} \dot{e} \\ \dot{\hat{f}} \end{bmatrix} = A_e \begin{bmatrix} e \\ \hat{f} \end{bmatrix} - \begin{bmatrix} N \\ 0 \end{bmatrix} f \quad (19)$$

in the case of system (8) with unknown inputs or nonlinearities. From (17) the following result can be obtained [23].

3.3 Known System without external inputs

Theorem 1. If the pair (A, C) is observable, then there exists a PI-observer with any dynamics for the system (7), such that $\lim_{t \rightarrow \infty} [\hat{x}(t) - x(t)] = 0$ for any initial states $x(0)$, $\hat{x}(0)$ and $\hat{f}(0)$.

Proof. From the dynamics (17) of PI-observer it can be seen that the dynamics or poles of (17) can be arbitrarily assigned if and only if the matrix pair $\left(\begin{bmatrix} A & L_3 \\ 0 & 0 \end{bmatrix}, [C \ 0] \right)$ is observable, i.e.

$$\text{rank} \left\{ \begin{bmatrix} sI - A - L_3 & \\ 0 & sI \\ C & 0 \end{bmatrix} \right\} = n + \dim(\hat{f}) \quad (20)$$

holds for all $s \in \mathbf{C}$. Furthermore, the condition (19) is equivalent to

$$\text{rank} \left\{ \begin{bmatrix} A & L_3 \\ C & 0 \end{bmatrix} \right\} = n + \dim(\hat{f}) \quad (21)$$

when $s = 0$ and

$$\text{rank} \left\{ \begin{bmatrix} sI - A \\ C \end{bmatrix} \right\} = n \quad (22)$$

when $s \neq 0$. The condition (21) implies that the dimension of the integrator must be less than or equal to that of the outputs. Since the matrix L_3 may be arbitrarily selected, the rank condition (22) holds if and only if

$$\text{rank} \left\{ \begin{bmatrix} A \\ C \end{bmatrix} \right\} = n \quad (23)$$

Combining the conditions (22) and (23) leads to

$$\text{rank} \left\{ \begin{bmatrix} sI - A \\ C \end{bmatrix} \right\} = n \quad (24)$$

for all $s \in \mathbf{C}$, i.e. (A, C) is observable.

A main motivation to study the PI-observer is to reconstruct the states of the system (8) with nonlinearities. The following two theorems give the results in case of the system (8).

3.4 Known Systems with Constant External Inputs

Theorem 2. Assume that $\lim_{t \rightarrow \infty} f(x, u, t)$ exists. Then, there exists a PI-observer with any dynamics for the system (8), such that $\lim_{t \rightarrow \infty} [\hat{x}(t) - x(t)] = 0$ for any initial states $x(0)$, $\hat{x}(0)$ and $\hat{f}(0)$ if (A, C) is observable and

$$\text{rank} \left\{ \begin{bmatrix} A & N \\ C & 0 \end{bmatrix} \right\} = n + r_1 \quad (25)$$

Proof. Using the construction method, we prove Theorem 2. Let $L_3 = N$. Then, the dynamics (19) of the estimation error of PI-observer (17) becomes

$$\begin{bmatrix} \dot{e} \\ \dot{\hat{f}} \end{bmatrix} = A_e \left\{ \begin{bmatrix} e \\ \hat{f} \end{bmatrix} - \begin{bmatrix} 0 \\ I \end{bmatrix} f \right\} \quad (26)$$

where $A_e = \begin{bmatrix} A - L_1 C & N \\ -L_2 C & 0 \end{bmatrix}$. Similarly with the proof of Theorem 1, the eigenvalues of the matrix A_e can be arbitrarily assigned by the matrices L_1 and L_2 if and only if the matrix pair $\left(\begin{bmatrix} A & N \\ 0 & 0 \end{bmatrix}, [C \ 0] \right)$ is observable, i.e.

$$\text{rank} \left\{ \begin{bmatrix} sI - A - N \\ 0 & sI \\ C & 0 \end{bmatrix} \right\} = n + r_1 \quad (27)$$

holds for all $s \in \mathbf{C}$. This condition is equivalent to

$$\text{rank} \left\{ \begin{bmatrix} A & N \\ C & 0 \end{bmatrix} \right\} = n + r_1 \quad (28)$$

when $s = 0$ and

$$\text{rank} \left\{ \begin{bmatrix} sI - A \\ C \end{bmatrix} \right\} = n \quad (29)$$

when $s \neq 0$. This implies that under the conditions in theorem 2 the dynamics of PI-observer (16) for the system (8) can be arbitrarily assigned. Therefore, the eigenvalues of A_e can be arbitrarily placed at any locations in the left-half complex plane when the conditions in theorem 2 are satisfied. This means that the dynamics (26) is stabilizable by means of the matrices L_1 and L_2 . When the dynamics (26) is asymptotically stable, its solution will converge to the equilibrium. Then, from (26) it can be easily seen that

$$\lim_{t \rightarrow \infty} \begin{bmatrix} e(t) \\ \hat{f}(t) \end{bmatrix} = \begin{bmatrix} 0 \\ \lim_{t \rightarrow \infty} f(x, u, t) \end{bmatrix} \quad (30)$$

3.5 Known Systems with Arbitrary External Inputs

Theorem 3. Assume that $f(x, u, t)$ is bounded. Then, there exists a high-gain PI-observer for the system (8) such that $\hat{x}(t) - x(t) \rightarrow 0$ ($t > 0$) for any initial states $x(0)$, $\hat{x}(0)$ and $\hat{f}(0)$ if

- 1) (A, C) is observable, which includes

$$\text{rank} \left\{ \begin{bmatrix} C \\ CA \\ \vdots \\ CA^{k-1} \end{bmatrix} \right\} = n \quad , \quad (31)$$

where k is the observability index of (A, C) ,

- 2) $\text{rank} \left\{ \begin{bmatrix} A & N \\ C & 0 \end{bmatrix} \right\} = n + r_1$; and
 3) $CN = 0$

Proof. Let $L_3 = N$. Then, analogously with the proof of theorem 2, it is easily verified that the dynamics of PI-observer (17) for the system (8) can be arbitrarily assigned by means of the matrices L_1 and L_2 if the conditions 1) and 2) in theorem 3 are satisfied.

Under the selection of L_3 the dynamics (19) of the estimation error becomes (26). When A_e is stable, the solution to (26) will be also bounded if $f(x, u, t)$ is bounded. Let $\begin{bmatrix} L_1 \\ L_2 \end{bmatrix} = \rho_1 \begin{bmatrix} \tilde{L}_1 \\ \tilde{L}_2 \end{bmatrix}$. Then, (26) may be written as

$$\frac{1}{\rho_1} \begin{bmatrix} \dot{e} \\ \dot{\hat{f}} \end{bmatrix} = \frac{1}{\rho_1} \begin{bmatrix} A & N \\ 0 & 0 \end{bmatrix} \begin{bmatrix} e \\ \hat{f} \end{bmatrix} - \begin{bmatrix} \tilde{L}_1 \\ \tilde{L}_2 \end{bmatrix} C e - \frac{1}{\rho_1} \begin{bmatrix} N \\ 0 \end{bmatrix} f \quad (32)$$

From (32) it follows that

$$C e = 0 \quad (33)$$

for $\rho \rightarrow \infty$. Differentiating (33) and using (19) give

$$C \dot{e} = C(A - L_1 C)e + CN(\hat{f} - f) \quad (34)$$

From the condition 3) and (33) we have

$$C A e = 0 \quad . \quad (35)$$

In the same way under the condition 1) we can obtain

$$C A^i e = 0 \quad i = 0, 1, \dots, k - 1 \quad (36)$$

Then from (33), (35) and (36) it follows that

$$e = 0 \quad (37)$$

due to condition 1). Substituting (37) into (19) gives

$$\hat{f} - f = 0 \quad (38)$$

because of the full-column rank of N . Equations (37) and (38) mean that the estimates \hat{x} and \hat{f} of the PI-observer (19) converge to the states x and the unknown inputs f of the system (8) when ρ_1 goes to the infinity. This shows that \hat{x} and \hat{f} may approximate x and f in the case of high gains.

In [23], [25] furthermore it is shown, that this type of observer also can be applied in general to systems not completely known with unknown additive inputs. In contrast to the mentioned works in the meantime the condition for the application of the PI-Observer to such structures is corrected to the conditions

$$\rho_1 \rightarrow \infty \quad \text{and} \quad (39)$$

$$\frac{\rho_2}{\rho_1} \rightarrow \infty \quad \text{with} \quad L_3 = \rho_2 N. \quad (40)$$

which gives theoretical hints to understand the observed success of the observer technique in robotics and machine-dynamics. In this application the PIO is applied to known systems with arbitrary external inputs.

4 Modeling and Simulation

Figure 4 illustrates the system to be considered: a torsion-stiff wheelset with linear springs c_{wh} , c_{wv} and dampers d_{wh} , d_{wv} for horizontal and vertical degrees of freedom. The electric drive is coupled with an elastic torsion spring-damper combination c_{MW} , d_{MW} to the wheelset. The other constants are the motor inertia Θ_M , the rotational inertia of the wheelset and drive Θ_W , and the related mass of the wheelset m_W . The modeled degrees of freedom are the motor angle φ_M , the wheel angle φ_W , the horizontal displacement of the wheelset u_{wx} and the vertical displacement of the wheelset u_{wz} . Modeled, but not given in the illustration fig. 4 are also the modal displacements of the rail u_{g1} , u_{g2} and the angles for the spatial orientation of the wheelset φ_1 , φ_2 .

The equations of motion are given by

$$\ddot{\varphi}_M + \frac{d_{MW}}{\Theta_M}(\dot{\varphi}_M - \dot{\varphi}_W) + \frac{c_{MW}}{\Theta_M}(\varphi_M - \varphi_W) = M(t) \quad (41)$$

$$\ddot{\varphi}_W + \frac{d_{MW}}{\Theta_M}(\dot{\varphi}_W - \dot{\varphi}_M) + \frac{c_{MW}}{\Theta_M}(\varphi_W - \varphi_M) = \frac{2rT_\xi}{\Theta_W} \quad (42)$$

$$\ddot{u}_{wx} + \frac{2d_w}{m_w}\dot{u}_{wx} + \frac{2c_w}{m_w}u_{wx} = \frac{2T_\xi}{m_w} \quad (43)$$

$$\ddot{u}_{wz} + \frac{2d_w}{m_w}\dot{u}_{wz} + \frac{2c_w}{m_w}u_{wz} = \frac{2N}{m_w} - g \quad (44)$$

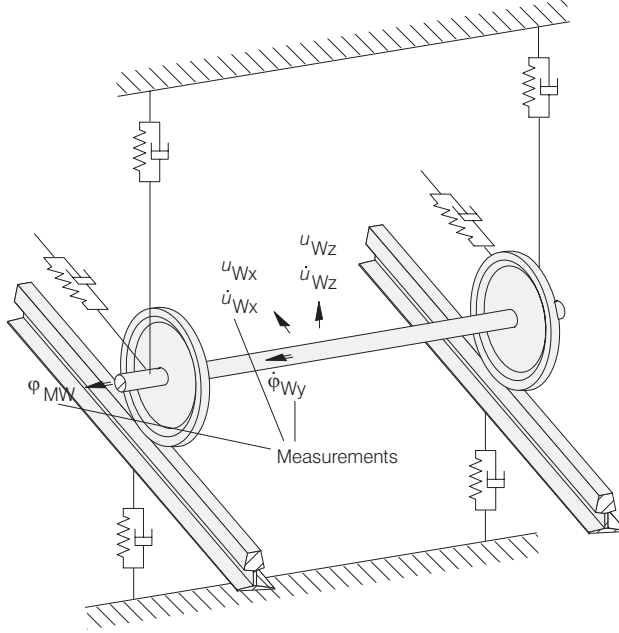


Fig. 4. Illustration of the wheelset to be considered

with the time-dependent normal contact load N , \dot{N} . The equations are coupled with the equations for the (modal) rail vibration and mainly due to the kinematic equations for the tangential contact force. The corresponding equation for the slip η is in absence of the absolute velocity of the bogie in the shown simulation example

$$\eta = 1 - \frac{\dot{\varphi}_W}{\dot{\varphi}_M} - \frac{\dot{u}_{wx}}{r\dot{\varphi}_M}. \quad (45)$$

This definition denotes some kind of averaging slip, and has to be used without loss of generality to get not only the elastic slip considering the elastic horizontal displacement of the wheelset. For practical purposes (with the possibility to measure the absolute speed) the usual definitions using the absolute speed v_0 can be used.

It should be noted, that there also exists a kinematical coupling between the rail, the elastic contact and the disturbance height Δz

$$d = u_{g1} + u_{g2} - u_{wz} + \Delta z \quad (46)$$

of the rail. For the following simulations Δz (as a stochastic value) works as an excitation. The whole model results as a nonlinear system with 10 elastic degrees of freedom. The main features of this model are taken from [13].

To get realistic adhesion characteristics the friction coefficient μ is stochastically modified. So a much more realistic characteristic as given by the Shen-Hedrick-Elkins model (4)–(6) as shown in Fig. 5 is available.

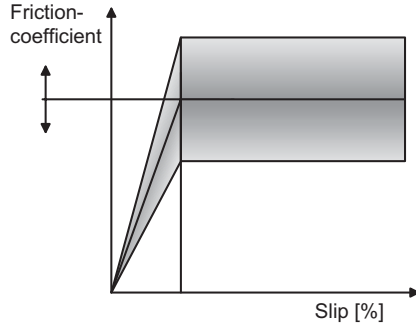


Fig. 5. Adhesion characteristic with stochastically modified friction coefficient

It should be noted that the PIO-design is independent from this structural and parametrical information. For the PIO only the known parts of (41)–(43) are used, the parts including T_ξ and the other equations are only used for the system simulation model.

4.1 Simulation Results

For the simulations the input is the torque $M(t)$ as a step function. In Fig.6 the results for $M(t) = 5 \cdot 10^4$ Nm and for the PI-Observer using the two measurements φ_M and u_{wx} are depicted. The upper plot shows the time behavior of the tangential contact force T_ξ (marked as o) and its estimation (marked as +). Then the adhesion characteristic – that is T_ξ/N depending on the slip η – is shown. Here the absolute value of η is used to get the rolling condition $\eta = 1$ with the used slip definition (45). This first plot shows that the observer works very well in the case of using two measurements.

Next the observer is used with only the measurement of φ_M and the same torque size as in the first simulation. Fig. 7 shows the results of that simulation. Again the estimation of the time behavior of the contact force works quite well but the adhesion characteristic is only roughly estimated.

For the same settings as in the first simulation but with a torque twice as there the results are given in Fig. 8. This shows that the success is independent of the height of the input.

The applied torque for the following simulations is again $M(t) = 5 \cdot 10^4$ Nm. For an observer with two measurements with additional noise the results of the simulation are shown in Fig. 9. The estimation of the time behavior as well as the estimation of the adhesion characteristic is close to the real run of the curve.

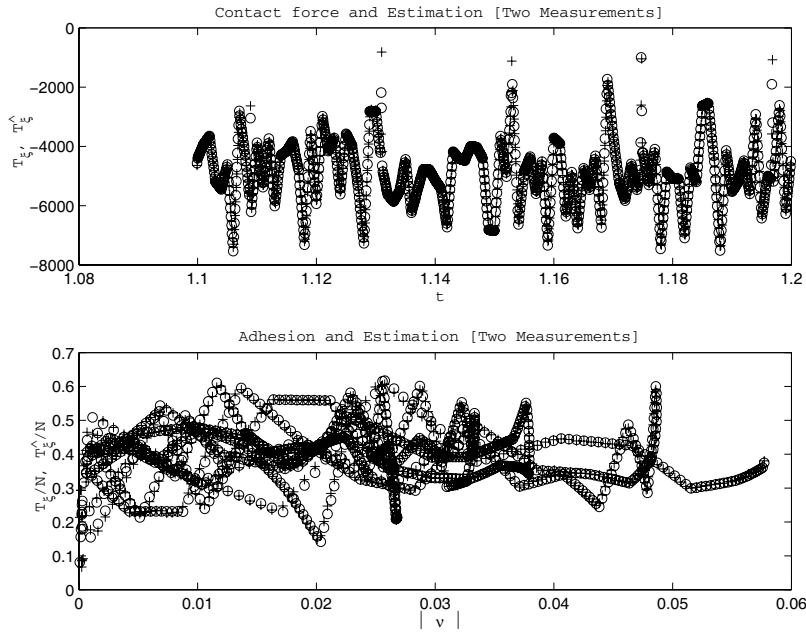


Fig. 6. a) Time behavior of the contact force and b) adhesion characteristic

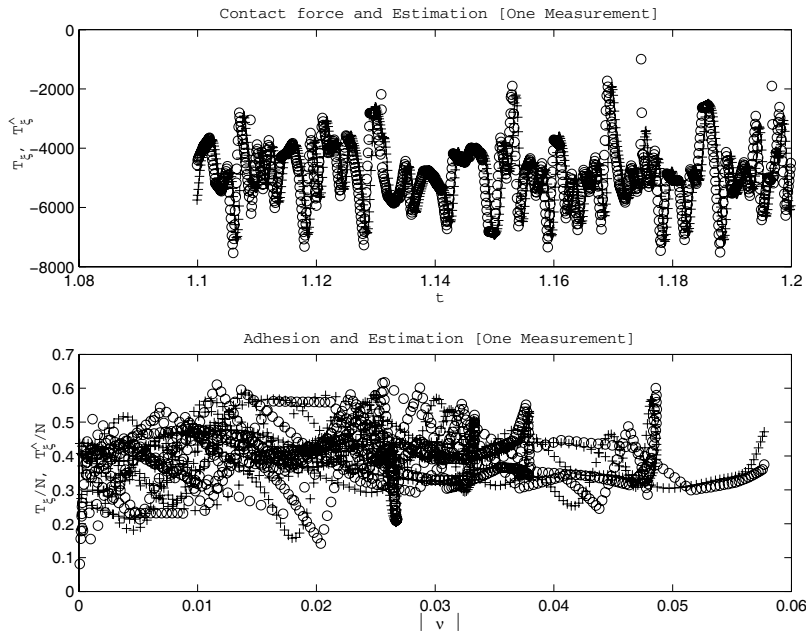


Fig. 7. a) Time behavior of the contact force and b) adhesion characteristic

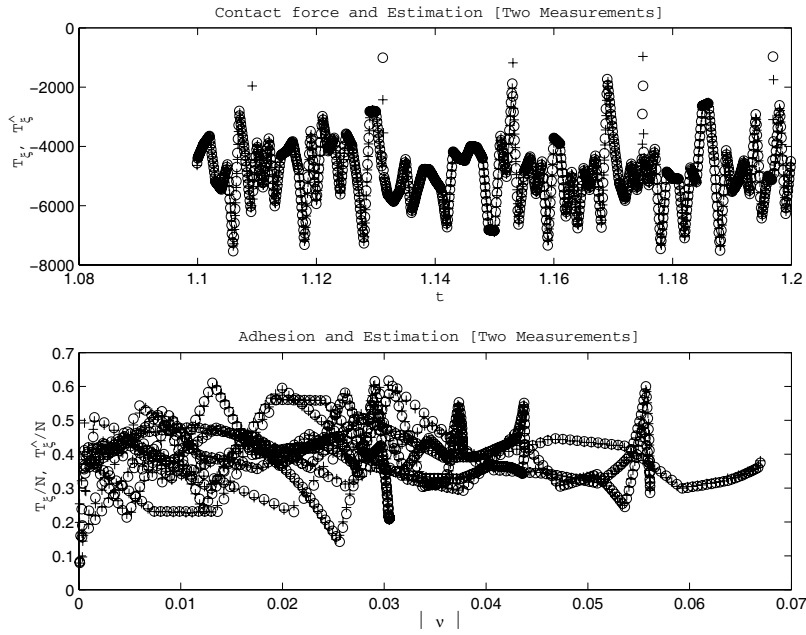


Fig. 8. a) Time behavior of the contact force and b) adhesion characteristic

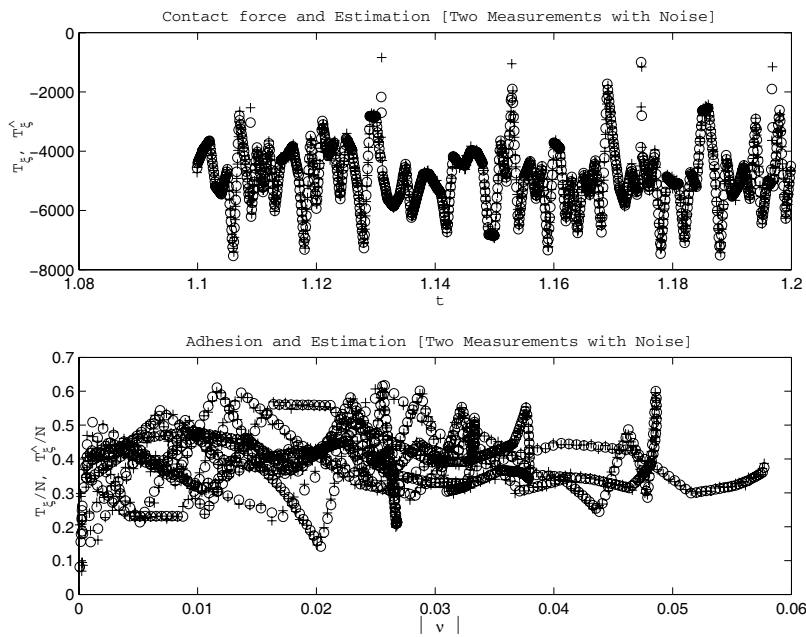


Fig. 9. a) Time behavior of the contact force and b) adhesion characteristic

Figure 10 shows the result for an observer with two measurements with higher noise than shown in the results given with Fig. 9. An additional difference to the case before is the consideration of a shorter time slice of the simulation. This resolution displays less good estimations of the curves.

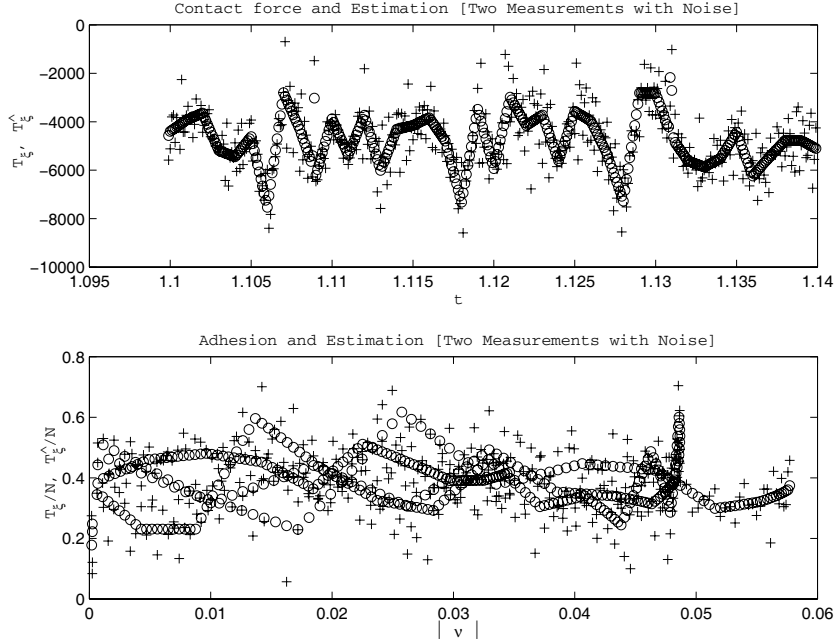


Fig. 10. a) Time behavior of the contact force and b) adhesion characteristic

5 Concluding Remarks and Future Aspects

In this contribution the application of the Proportional-Integral Observer (PIO) for model-based model validation purposes within the rail-wheel-subgrade modeling is shown. As a first example the reconstruction of the contact behavior (usually modeled by contact models) is realized and therefore a scheme for contact model validation is implemented. Using a theoretical model of an elastic supported wheelset with a nonlinear contact model it can be shown by simulations that the linear PIO-scheme is able to estimate the nonlinear tangential contact forces. This inside view into the unmeasurable contact situation gives the base for advanced adhesion control strategies. The next step is to replace the simulation model by a real system and to compare the observer values originated with real measurements with the model

values of the model to be validated. In other applications this comparison shows satisfying result [1].

Further as an other example the detection of voids within the subsoil is aimed. In this additional application the observer estimates the stiffness coefficients within the subsoil with the aid of measurements of the normal forces and the sleeper angle.

Acknowledgement

This work is a first result from the sub-project 'Contact, Friction, Wear' of the DFG-Priority-Program 'System Dynamics and Long-term Behavior of Vehicle, Track and Subgrade'. The authors wish to express their thanks to the DFG for the support.

References

1. Abicht, C.; Bormann, J.; Müller, P.C.; Söffker, D.; Ulbrich, H. (2001) Model-Based Estimation of Impact Forces affecting Elastic Structures: Simulation and Experiment. Proc. 18th ASME-DECT Biennial Conference on Mechanical Vibration and Noise, Symposium on Vibration Including Friction and Impacts, Pittsburgh, Pennsylvania, USA, September 9-13, 2001, 6 pages
2. Ackermann, J. (1989) Positionsregelung reibungsbehafteter elastischer Industrieroboter. VDI-Fortschrittberichte, Reihe 8, Nr. 180, VDI-Verlag, Düsseldorf
3. Anderson, B.D.O.; Moore, J.B. (1989) Optimal Control - Linear Quadratic Methods. Prentice Hall, New York
4. Buscher, M.; Pfeiffer, R.; Schwartz, H.J. (1993) Radschlupfregelung für Drehstromlokomotiven. eb - Elektrische Bahnen 91, 1993, Seiten 163-178
5. Hahn, K.; Hase, K.R.; Sommer, H. (1993) Fortschritte bei der Kraftschlußausnutzung für die Hochgeschwindigkeits- und Schwerlasttraktion. ETR 42, 1993, Seiten 67-74
6. Hertz, H. (1882) Über die Berührung fester, elastischer Körper und über die Härte. Verhandlungen des Vereins zur Förderung des Gewerbefleißes, Leipzig, Nov. 1882
7. Hou, M.; Müller, P.C. (1992) Design of Observers for Linear Systems with Unknown Inputs. IEEE Trans. Aut. Control, Vol. 37, 1992, pp. 871-875
8. Johnson, C.D. (1976) Theory of Disturbance-Accommodating Controllers. In: Leondes, C.T. (Ed.): Control and Dynamic Systems. Academic Press, Vol. 12, 1976, pp. 387-489
9. Kalker, J.J. (1990) Three-Dimensional Elastic Bodies in Rolling Contact. Kluwer Academic Publishers. Dordrecht, Boston, London
10. Kalker, J.J.; Dekking, F.M.; Vollebregt, E.A.H. (1997) Simulation of Rough, Elastic Contacts. Journal of Applied Mechanics, Vol. 64 (1997), pp. 361-368
11. Knothe, K. (1992) Lateraldynamik von Schienenfahrzeugen. Vorlesungsskript TU Berlin, Wintersemester 1992/93
12. Lang, W.; Roth, G. (1996) Optimale Kraftschlußausnutzung bei Hochleistungs-Schienenfahrzeugen. ETR 42, 1996, Seiten 61-66

13. Lange, M.; Groß-Thebing, A.; Stiebler, M.; Knothe, K. (1995) Simulationsmodell für Vollbahn-Antriebssysteme zur Untersuchung der ausnutzbaren Zugkraft. Arbeitsbericht zum DFG-Forschungsvorhaben Kn/St 132/20, 1993 bis 1995
14. Lurje, A.I. (1963) Räumliche Probleme der Elastizitätstheorie. Akademie Verlag, Berlin
15. Neumann, R.; Moritz, W., (1990) Observer-based joint controller design for a robot for space operation. In: Proc. Eight CISM-IFTOMM Symp. Theory of Robots and Manipulators, Ro.Man.Sy, Krakau, Poland, July 1990
16. Müller, P.C.; Lückel, J. (1977) Zur Theorie der Störgrößenaufschaltung in linearen Mehrgrößenregelsystemen. Regelungstechnik, 25, 1977, Seiten 54-59
17. Müller, P.C. (1989) Indirect Measurement of Nonlinear Effects by State Observers. IUTAM Symposium on Nonlinear Dynamics in Engineering Systems, University of Stuttgart, FRG, Aug. 21-25, 1989
18. Ripke, B. (1995) Hochfrequente Gleismodellierung und Simulation der Fahrzeug-Gleis-Dynamik unter Verwendung einer nichtlinearen Kontaktmechanik. VDI-Fortschrittberichte, Reihe 12, Nr. 249, Düsseldorf
19. Schreiber, R.; Kögel, R. (1996) Identifikationsmethode zur Bestimmung der Adhäsion zwischen Rad und Schiene. ZEV+DET Glas. Ann. 120, 1996, Seiten 48-54
20. Shen, Z.Y.; Hedrick, J.K.; Elkins, J.A. (1983) A comparison of alternative creep force models for rail vehicle dynamic analysis. Proc. of 8th IASVD Symposium, MIT, Cambridge, August 15-19, 1983
21. Stiebler, M.; Knothe, K.; Dreimann, K. (Hrsg.) (1996) Tagungsband des Workshops 'Simulation und Praxis der Kraftschlußausnutzung von Hochleistungs-Triebfahrzeugen. Berlin, 27./28. Juni 1996
22. Söffker, D.; Bajkowski, J.; Müller, P.C. (1993) Crack Detection in Turbo Rotors - A New Observer - Based Method. ASME Journal of Dynamic Systems, Measurements, and Control, 3, 1993, pp. 518 - 524
23. Söffker, D.; Yu, T.J., Müller, P.C. (1995) State Estimation of Dynamical Systems with Nonlinearities by using Proportional - Integral Observer. International Journal of System Science. Vol. 26, 1995, No. 9, pp. 1571-1582
24. Söffker, D. (1995b) A New Model - Based Tool for Failure Detection and Isolation in Machine- and Rotordynamics. Proc. ASME 12th RSAFP Conf., Sept. 1995, Boston, USA
25. Söffker, D. (1996) Zur Modellbildung und Regelung längenvariabler, elastischer Roboterarme. Dissertation Universität-GH Wuppertal 1995, auch als: VDI-Fortschrittberichte, Reihe 8, Nr. 584, 1996
26. Söffker, D. (1999) Observer-based measurement of contact forces of the nonlinear rail-wheel contact as a base for advanced traction control. In: Wallaschek, J., Lückel, J., Littmann, W. (Eds.) Mechatronics and Advanced Motion Control, HNI-Verlagsschriftenreihe, Band 49, pp. 305-320
27. Zhang, J.; Knothe, K. (1995) Berechnungsmodell für Tangentialschlupfkkräfte beim Kontakt in der Hohlkehle. ILR-Mitteilung 294 (1995), Institut für Luft- und Raumfahrt, TU Berlin, 1995

Index

- abstract, 1
- contact modeling, 3
- disturbance model, 5
- Extended Kalman Filter, 4
- extended linear model, 6
- general system description, 5
- Hertz normal-contact, 3
- Kalker theory, 3
- Luenberger observer, 4
- Luenberger observer extension, 6
- optimal contact use, 1
- PIO, 4
- robust estimation of unknown inputs, 4
- Shen-Hedrick-Elkins model, 3
- structure of the PIO, 6
- Unknown Input Observer, 4
- virtual measurement device, 2
- void detection, 17